

AD

AD-E403 124

Technical Report ARAET-TR-07010

**THEORETICAL STUDIES AND EXPERIMENTAL VALIDATION FOR GENERATING
CONCENTRATION DISTRIBUTIONS ACROSS THE PROPELLANT GRAIN UPON
SHEAR-INDUCED PARTICLE MIGRATION DURING EXTRUSION**

David Fair
Donald Chiu
Sam Moy
ARDEC

Dilhan M. Kalyon
M. Allende
Stevens Institute of Technology
Castle Point on Hudson
Hoboken, NJ 07030

June 2007



ARMAMENT RESEARCH, DEVELOPMENT AND
ENGINEERING CENTER

Armaments Engineering & Technology Center

Picatinny Arsenal, New Jersey

Approved for public release; distribution is unlimited.

The views, opinions, and/or findings contained in this report are those of the author(s) and should not be construed as an official Department of the Army position, policy, or decision, unless so designated by other documentation.

The citation in this report of the names of commercial firms or commercially available products or services does not constitute official endorsement by or approval of the U.S. Government.

Destroy this report when no longer needed by any method that will prevent disclosure of its contents or reconstruction of the document. Do not return to the originator.

REPORT DOCUMENTATION PAGE				Form Approved OMB No. 0704-01-0188	
<p>The public reporting burden for this collection of information is estimated to average 1 hour per response, including the time for reviewing instructions, searching existing data sources, gathering and maintaining the data needed, and completing and reviewing the collection of information. Send comments regarding this burden estimate or any other aspect of this collection of information, including suggestions for reducing the burden to Department of Defense, Washington Headquarters Services Directorate for Information Operations and Reports (0704-0188), 1215 Jefferson Davis Highway, Suite 1204, Arlington, VA 22202-4302. Respondents should be aware that notwithstanding any other provision of law, no person shall be subject to any penalty for failing to comply with a collection of information if it does not display a currently valid OMB control number.</p> <p>PLEASE DO NOT RETURN YOUR FORM TO THE ABOVE ADDRESS.</p>					
1. REPORT DATE (DD-MM-YYYY) June 2007		2. REPORT TYPE		3. DATES COVERED (From - To)	
4. TITLE AND SUBTITLE THEORETICAL STUDIES AND EXPERIMENTAL VALIDATION FOR GENERATING CONCENTRATION DISTRIBUTIONS ACROSS THE PROPELANT GRAIN UPON SHEAR-INDUCED PARTICLE MIGRATION DURING EXTRUSION			5a. CONTRACT NUMBER W15QKN-05-D-0011		
			5b. GRANT NUMBER		
			5c. PROGRAM ELEMENT NUMBER		
			5d. PROJECT NUMBER		
6. AUTHORS D. Fair, D. Chiu, and S. Moy, ARDEC D. M. Kalyon and M. Allende, Stevens Institute of Technology			5e. TASK NUMBER Task Order 2		
			5f. WORK UNIT NUMBER		
7. PERFORMING ORGANIZATION NAME(S) AND ADDRESS(ES) U.S. Army ARDEC, AETC Stevens Institute of Technology Energetics, Warheads & Environmental Castle Point on Hudson Technology (AMSRD-AAR-AEE-W) Hoboken, NJ 07030 Picatinny Arsenal, NJ 07806-5000			8. PERFORMING ORGANIZATION REPORT NUMBER		
9. SPONSORING/MONITORING AGENCY NAME(S) AND ADDRESS(ES) U.S. Army ARDEC, EM Technical Research Center (AMSRD-AAR-EMK) Picatinny Arsenal, NJ 07806-5000			10. SPONSOR/MONITOR'S ACRONYM(S)		
			11. SPONSOR/MONITOR'S REPORT NUMBER(S) Technical Report ARAET-TR-07010		
12. DISTRIBUTION/AVAILABILITY STATEMENT Approved for public release; distribution is unlimited.					
13. SUPPLEMENTARY NOTES					
14. ABSTRACT The theory of the shear-induced particle migration is presented with numerical simulation results from multiple geometries using Poiseuille flow in a rectangular die. It appears that the functionally-grading of propellant strands can be generated upon shear-induced particle migration in propellant extrusion. The theory and the results obtained in this study with an inert simulant formulation demonstrate the utilities of the suggested methodologies and their practicality.					
15. SUBJECT TERMS Functionally graded propellant Shear-induced migration Poiseuille flow Couette flow Burn rate gradients					
16. SECURITY CLASSIFICATION OF:			17. LIMITATION OF ABSTRACT SAR	18. NUMBER OF PAGES 28	19a. NAME OF RESPONSIBLE PERSON D. Fair, D. Chiu, and S. Moy
a. REPORT U	b. ABSTRACT U	c. THIS PAGE U			19b. TELEPHONE NUMBER (include area code) (973) 724-2941

CONTENTS

	Page
Executive Summary	1
Introduction and Objectives	1
Background and Introduction to Shear Induced Migration	1
Discussion	5
Method 1: Flow in Between Two Cylinders with a Wide Gap in Between and with One of the Cylinders Rotating and the Other Stationary	5
Method 2: Generation of Concentration Distributions Using Pressure-driven Flows Through Dies	9
Selection of the Binder	11
Experimental Studies Using a Simulant and a Slit Die	12
Materials	12
Processing	12
Slit Die for Assessing the Migration Effects	13
Collection of the Sample	16
Microscopy of the Sample and Further Analysis to Follow	16
Scanning Electron Microscopy Analysis of the Extruded Samples	17
Ramifications	20
Future Work	20
References	21
Distribution List	23

FIGURES

1	Contour plot of model results for burning rate (cm/s) at 125 MPa	4
2	Wide gap Couette geometry	5
3	Steady state concentration distribution for wide gap Couette flow	6
4	Transient concentration distributions as function of inner cylinder revolutions	7
5	Burn rate versus location in the propellant to be recovered from the annular gap between the two cylinders of figure 4 upon Couette flow	8
6	Predicted concentration distribution for a 50% suspension at various particle radius to gap width ratios	9

FIGURES
(continued)

	Page
7 Flow through a rectangular slit of gap, H, or a circular tube with radius R	9
8 Fully developed concentration distribution for steady state Poiseuille flow	11
9 Particle concentration distributions for a 45% suspension and at various capillary length to diameter ratios	12
10 50% PDMS_50% ceramic microsphere by volume batch mixing at 30 rpm, 210 cm ³ for 10 min	13
11 Adjustable gap rheometer	14
12 Cartridge	14
13 Instron slit rheometer	15
14 50% PDMS and 50% ceramic microsphere by volume at 0.1 in./min crosshead speed	15
15 50% PDMS_50% ceramic microsphere by volume	16
16 50% PDMS_50% ceramic microsphere by volume	16
17 50% PDMS_50% ceramic microsphere by volume	17
18 SEM image I - core of the extrudates: away from the wall	17
19 SEM image II - core of the extrudates: away from the wall	18
20 SEM image III - skin of the extrudates: at the wall	18
21 SEM image IV - skin of the extrudates: at the wall	19
22 SEM image V - skin of the extrudates: at the wall	19
23 SEM image VI - skin of the extrudates: at the wall	20

EXECUTIVE SUMMARY

In this final report, the theory of the shear-induced particle migration is presented in conjunction with typical numerical simulation results using multiple geometries, along with data collected using Poiseuille flow in a rectangular die. It appears that the functionally-graded propellant strands can be generated upon shear-induced particle migration in extrusion provided that:

1. One uses the greatest particle diameter, which can be acceptable to the program
2. In pressure driven flow the longest length possible is used
3. A Newtonian binder, which is to be either thermosetting or thermoplastic, is employed

The theory and the results obtained with an inert simulant formulation demonstrate the utilities of the suggested methodologies and their practicality. It is anticipated that this preliminary, modest study will be followed with additional funding to seek the opportunity to render this technology available to U.S. Army for generating fast/slow burn propellants at a fraction the cost of current methodologies that are also being investigated for their suitability.

INTRODUCTION AND OBJECTIVES

A feasibility study project was requested by the U.S. Army Armament Research, Development and Engineering Center (ARDEC), Picatinny Arsenal, New Jersey in order to demonstrate a novel processing technique for the manufacturing of a cross-sectional controlled burn rate advanced propellant for the purpose of improving ballistic efficiency. An integrated product team (IPT) was established for this project. This team consists of members from various competencies within the Armament Engineering Technology Center [AETC, (ARDEC)] and Stevens Institute of Technology (SIT). The objective of the work is for SIT to provide ARDEC with the results of a mathematical model of shear-induced particles migration during the processing and extrusion of some selected simulant compositions and some experimental validation. In the following, the background and the theory of particle migration are presented, along with some typical numerical simulation results and methodologies that can be employed, followed by the results of an experimental study.

BACKGROUND AND INTRODUCTION TO SHEAR INDUCED MIGRATION

Energetic materials like solid rocket fuels, gun propellants are suspensions consisting of a polymeric binder incorporated with rigid particles. The particles are generally symmetric with low aspect ratios and broad particle size distributions to allow achievement of relatively high solid packing ratios. The concentration of the rigid particles needs to be relatively high and in most cases approaches the maximum packing fraction of the solids (the characteristic concentration of the solid particles above which there is no fluidity). In the flow and processing of such highly filled suspensions, a number of mechanisms act to generate gradients in the concentrations of particles. For example, during pressure-driven Poiseuille flow (flow through circular tube dies or

rectangular slit dies) the binder can migrate in the axial direction i.e., flow direction. This behavior is observed especially with concentrated suspensions filled close to their maximum packing fractions and manifests itself as the filtration of the binder as a result of the imposed pressure gradient, superimposed on the bulk flow of the suspension.

The second type is the migration of the non-colloidal solid particles in inhomogeneous flows of the suspension in the transverse to flow direction; i.e., in the direction of the imposed deformation rate. When the Reynolds number is greater than 10^{-3} the inertial effects give rise to the radial migration of solid particles (refs. 1 and 2). However, the migration of the particles, and the resulting development of particle concentration gradients in transverse to flow direction occur upon inhomogeneous flows even in the absence of inertial effects. Thus, such migrations even occur during creeping flows in which the prevailing Reynolds number approaches zero. Since the shear viscosity of most energetic suspensions is very high the flow of energetic suspensions could be considered as creeping flow and thus subject to the migration of particles even in the absence of inertial effects.

The experimental evidence to the occurrence of the particle migrations in conditions where gradients of deformation rates exist under creeping flow conditions was first provided by Gadala-Maria and Acrivos (ref. 3) where the shear viscosity of concentrated suspensions were observed to decrease with time in Couette flow (coal suspensions). Leighton and Acrivos (ref.4) later showed that the observed decrease in viscosity was associated with the migration of solid particles from the high shear rate region located in between the two concentric cylinders to the low shear rate region located at the reservoir bottom of the Couette geometry.

The migration of particles from high shear rate to low shear rate was further documented in wide-gap Couette flow (where shear rate is not uniform) by Abbott et al. (ref.5) using magnetic resonance imaging. Generally, the flow regions that experience relatively high rates of shear become depleted in particles and the flow regions that experience relatively low rates of shear become enriched in particles, thus giving rise to particle concentration distributions in the transverse to main flow direction.

A consequence of the shear-induced particle migration effect, which changes the concentration distribution in the channel, is the blunting of the velocity distribution. In pressure driven channel flow (rectangular slit and capillary) a number of investigators observed the blunting of the velocity profile (ref.6). As noted, such blunting is associated as being a consequence of particle concentration gradients that were indeed observed in channel flow by Koh et al. (ref. 7). Allende and Kalyon (ref. 8) showed that such particle migrations in pressure driven flows can occur if the particle radius over the channel gap is relatively high and also provided an additional experimental method to evaluate the importance of such migration.

Phenomenological models of migration of neutrally-buoyant, unimodal, and spherical particles suspended in Newtonian fluids, across planes of shear during non-homogeneous shear flows generally attribute the migration to irreversible interactions. By using scaling arguments, Leighton and Acrivos (ref. 4) were able to derive a general expression for the diffusive flux of particles in simple shear flow. Phillips et al. (ref. 9) used Leighton and Acrivos (ref. 4) flux expressions to develop a diffusion equation that describes the evolution of particle concentration distributions over time. This diffusion equation assumes that there are two primary causes for particle migration, i.e., particle interactions and local variations of the concentration-

dependent suspension viscosity. The Phillips et al. (ref. 9) model was further modified by Allende and Kalyon (ref. 8) by using two different boundary conditions, i.e. the continuity of the flux at the axis of symmetry and the incorporation of apparent slip at the wall (wall slip is prevalent in the flow of concentrated suspensions including energetic suspensions).

There are several ways in which the irreversible interactions can lead to particle migration in the presence of concentration and shear stress gradients. Following Phillips et al. (ref. 9), consider a suspension undergoing non-homogeneous shear flow. Within the plane of shear, the shear viscosity is constant. An interaction occurs when two particles embedded in adjacent shearing surfaces move past one another. Since these interactions may cause a particle to be irreversibly moved from its original streamline, a particle that experiences a higher interaction frequency from one direction than from the opposing direction will migrate normal to shearing surface and in the direction of the lower interactions frequency. This diffusion equation follows Leighton and Acrivos (ref. 4) and assumes that there are two primary causes for particle migration, i.e. gradients in collision frequency and gradients in suspension viscosity.

Consider a suspension of hard spheres with radius a in a Newtonian fluid with viscosity η_o . Assume that the particles diffuse in the Newtonian liquid at shear rate, $\dot{\gamma}$, with diffusivity D and that the Peclet number, $Pe = a^2 \dot{\gamma} / D$, is relatively large so that Brownian motion can be neglected. The number of collisions or interactions experienced by a particle scales as $\dot{\gamma} \phi$, where $\dot{\gamma}$ is the local shear rate and ϕ is the particle volume fraction. The gradient in the collision frequency over a characteristic distance of $O(a)$ is given by $a \bar{\nabla}(\dot{\gamma} \phi)$. Therefore, the particle flux \bar{N}_c , occurring due to a gradient in collision frequency, is given by [Phillips et al. (ref. 9)]

$$\bar{N}_c = -K_c a^2 \phi (\phi \bar{\nabla} \dot{\gamma} + \dot{\gamma} \bar{\nabla} \phi) \quad (1)$$

where K_c is a proportionality constant that needs to be determined from experimental data. The first term in equation 1 implies that even in the absence of a gradient, particle concentration migration of particles will result based on the non-homogeneous shear flow such as Poiseuille and wide-gap Couette flows. The second term in equation 1 states that a gradient in particle concentration will cause a spatial variation in the frequency of collisions. If a non-homogeneous shear flow is started in a suspension with a uniform concentration distribution, ϕ , the first term in equation 1 gives rises to a flux, which in turn generates a concentration gradient and hence induces a second flux proportional to $\bar{\nabla} \phi$. Thus, the two terms in equation 1 are, in general, in opposite directions. Particles migrate from regions of high to low shear rate and from regions of high to low concentration.

In addition to the flux caused by gradients in collision frequency, it is possible that an interaction between two particles will be affected by a gradient in suspension viscosity caused by the presence of gradients in the particle concentration. Both particles are displaced in the direction of lower viscosity. The magnitude of this displacement during each irreversible interaction is scaled with the relative change in suspension viscosity; i.e., $(a / \eta_s) \bar{\nabla} \eta_s$. If each interaction causes a displacement over a characteristic distance of $O(a)$ and the interaction frequency scales as $\dot{\gamma} \phi$, then the flux \bar{N}_η due to a viscosity gradient, is given by [Phillips et al. (ref. 9)]

$$\bar{N}_\eta = -K_\eta a^2 \frac{\dot{\gamma} \phi^2}{\eta_s} \bar{\nabla} \eta_s \quad (2)$$

where K_η is a diffusion constant that needs to be determined from experimental data, and $\eta_s = \eta_s(\phi)$ is the shear viscosity of the concentrated suspension. Phillips et al. (ref. 9) provided a conservation equation for solid particles, which can be written in a Lagrangian reference frame as

$$\frac{\partial \phi}{\partial t} + \bar{v} \cdot \bar{\nabla} \phi = -\bar{\nabla} \cdot (\bar{N}_c + \bar{N}_\eta) \quad (3)$$

Equation 3 is the shear-induced particle migration model developed by Phillips et al. (ref. 9) for a concentrated suspension of unimodal spheres undergoing non-homogeneous shear flows.

This model and its modifications by Allende and Kalyon (ref. 8) form the basis for the calculations to suggest that under certain conditions, distributions of particle concentrations will be generated. Earlier experimental work on burn rate determination has shown that changes in the concentrations of the energetic particles will lead to changes in burn rates. For example, the experimental work of Homan et al. (ref. 10) using energetic thermoplastic binders incorporated with RDX type nitramine particles has clearly shown that the burn rate of the energetic suspension would be a function of the concentration of particles as shown in figure 1 (figure 5 of ref. 10). The results clearly indicate that as the concentration of the RDX particles increases then the burn rate increases also across the entire range of particle sizes considered in the 2 to 32 μm size range. One can assume a relationship between the burn rate and the solids loading level as

$$\text{Burn rate} = c + b\phi + a\phi^2 \quad (4)$$

where ϕ is the volume fraction of RDX particles in the formulation and a , b , and c are constants that depend on the particle size, particle type/geometry, and the nature of the binder/particle interactions. Thus, the conditions that will generate particle concentration distributions will also lead to distributions of the burn rates. This forms the basis of the present project.

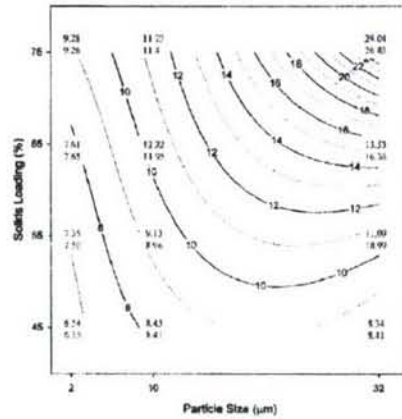


Figure 1
Contour plot of model results for burning rate (cm/s) at 125 MPa

There are two basic methodologies, which can be tested for the generation of propellants that exhibit location dependent distributions of energetic particles to give rise to propellant grains with multiple burn rates. These methodologies include the Couette flow and second the pressure driven die flow, both of which will be discussed next.

DISCUSSION

Method 1: Flow Between Two Cylinders With a Wide Gap in Between and With One of the Cylinders Rotating and the Other Stationary

Consider a concentrated suspension undergoing non-homogeneous shear flow in wide gap Couette flow geometry (fig. 2). In this graph, the non-dimensional inner cylinder radius, κ , was taken to be 0.2689. The inner cylinder with radius, κR , rotates with angular velocity, Ω , and outer cylinder with radius, R , is stationary, as shown in figure 2. The θ -component of the equation of motion in cylindrical coordinates yields

$$\frac{1}{r^2} \frac{\partial}{\partial r} (r^2 \tau_{r\theta}) = 0 \quad (5)$$

and the time-dependent evolution of the concentration profile can be obtained from the analysis for a transient Couette flow.

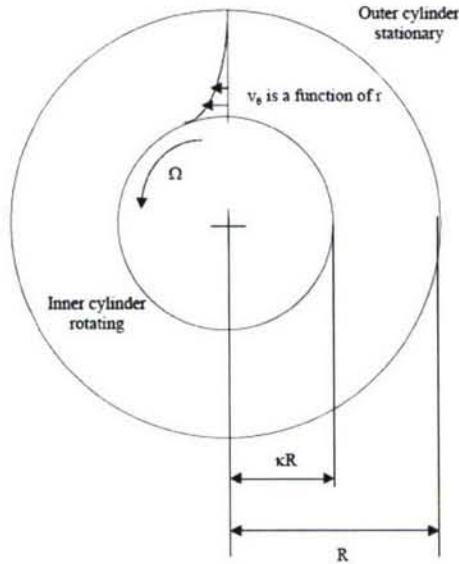


Figure 2
Wide gap Couette geometry

The analysis for a transient Couette flow requires the solution of equation 6 for the case $\phi = \phi(r, t)$, where r is the radial coordinate and t is time. The diffusion equation becomes

$$\frac{\partial \phi}{\partial t} = \frac{a^2}{r} \frac{\partial}{\partial r} \left\{ r \left[K_c \left(\phi^2 \frac{\partial \dot{\gamma}}{\partial r} + \dot{\gamma} \phi \frac{\partial \phi}{\partial r} \right) + K_\eta \frac{\dot{\gamma} \phi^2 \partial \eta_s}{\partial r} \right] \right\} \quad (6)$$

The θ -component of the equation of motion (eq 5) is solved to give an expression for the local shear rate, $\dot{\gamma}$, as a function of the concentration-dependent suspension viscosity, $\eta_s(\phi)$, which can be rendered a function of the volume fraction of the solids, ϕ , over the maximum packing fraction. The Krieger (ref. 11) model for example can be used to express the suspension viscosity, $\eta_s(\phi)$, as a function of the concentration, ϕ . Then, equation 6 is solved to give the concentration distribution $\phi = \phi(r, t)$.

The objective of such calculations is to determine the conditions of geometry, operating conditions, and the characteristics of the suspension that are necessary for the generation of the desired concentration distribution and hence burn rate distribution from one surface of the propellant to the other in the transverse direction.

The steady state distributions of the concentration for $K_c / K_\eta = 0.66$ are given in figure 3. These results suggest that if a concentrated suspension of energetic particles and/or binder is placed into the gap between two cylinders, one of which is rotating and the other is stationary, concentration gradients will be established with a high concentration of particles at the outer wall and a relatively low concentration of particles at the inner wall. The durations to reach these steady state concentration distributions will be a function of the particle radius over the gap ratio. The time-dependent development of the concentration distributions (as a function of the total number of rotations of the inner cylinder as shown in figure 3) for a particle radius over the gap ratio of 0.0194 for a concentrated suspension with a volume fraction loading level of 55% of particles by volume. The non-dimensional inner cylinder radius is $\kappa = 0.2689$. Experimental results shown are for 800 revolutions of the inner cylinder.

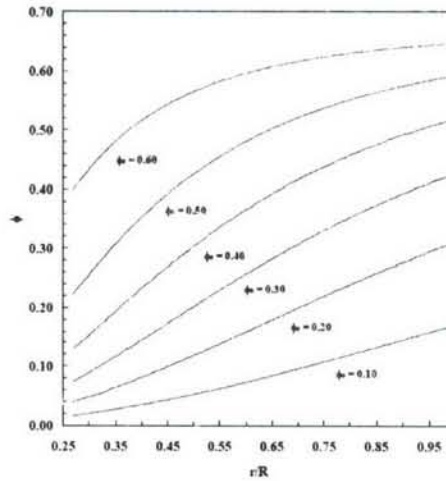


Figure 3
Steady state concentration distribution for wide gap Couette flow

Thus, this concentration profile would be achieved under conditions that involve a processing geometry, which follows a particle radius over the gap ratio of 0.02. The volume fraction of the rigid particles would be 55% by volume. **For a RDX mean particle radius of 75 μm , the gap in the Couette device to generate the particle concentration distribution given in figure 3 would be 3.8 mm.** The inner cylinder needs to be rotated 800 times under conditions that the propellant would not deteriorate and for which the temperature rise would not be significant. Heat transfer means can be provided through the surfaces of the two cylinders to allow the temperature to be kept at the targeted values. Upon generating the concentration profile by rotating the inner cylinder 800 times, the flow would be stopped and the structure would be frozen. For a thermosetting binder, this involves the curing of the propellant, preferably in situ, followed by removing of the cylinders and collecting the propellant slab lying in between the two cylinders. For thermoplastic binders (which melt and solidify upon reaching the melting temperature and upon the temperature being decreased to be less than the melting temperature of the polymer), the cylinders and hence the propellant in between the two cylinders would need to be quenched to again freeze in the concentration gradients that are generated. The outer cylinder needs to be splittable to allow the collection of the structured sample upon the completion of the structuring process upon shearing.

Assuming that the burn rate versus the concentration relationship given in equation 4 prevails under the conditions of a continuously varying concentration distribution and with values of $a = 50.5$, $b = -8.5$, and $c = 4$ for particles with a particle diameter of 150 μm and fitted from the volume fraction of solids range of 29 to 60% by volume of RDX. The slab of propellant with a slab thickness of 3.8 mm (to be recovered upon solidification from the annular space in Couette flow in between the two cylinders of figure 4, one of which is rotated 800 times) achieves a high rate of burn at one of its surfaces versus a low rate of burn at the other surface (fig. 5). The length of the propellant grain is equal to the length of the Couette geometry. The ratio of the burn rates achieved at the two surfaces is about three.

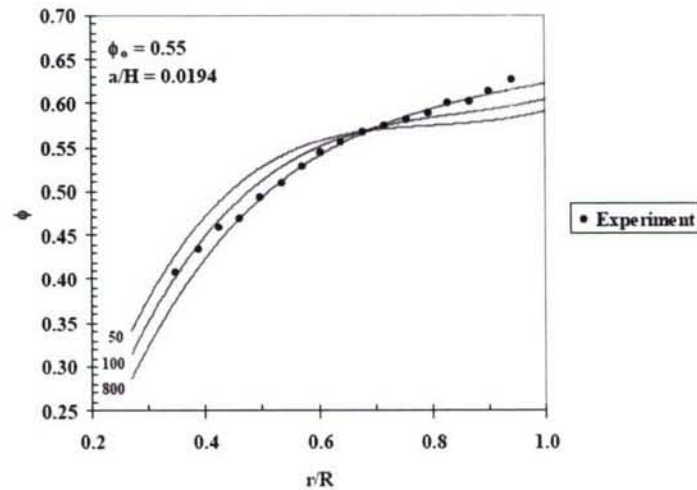


Figure 4
Transient concentration distributions as function of inner cylinder revolutions

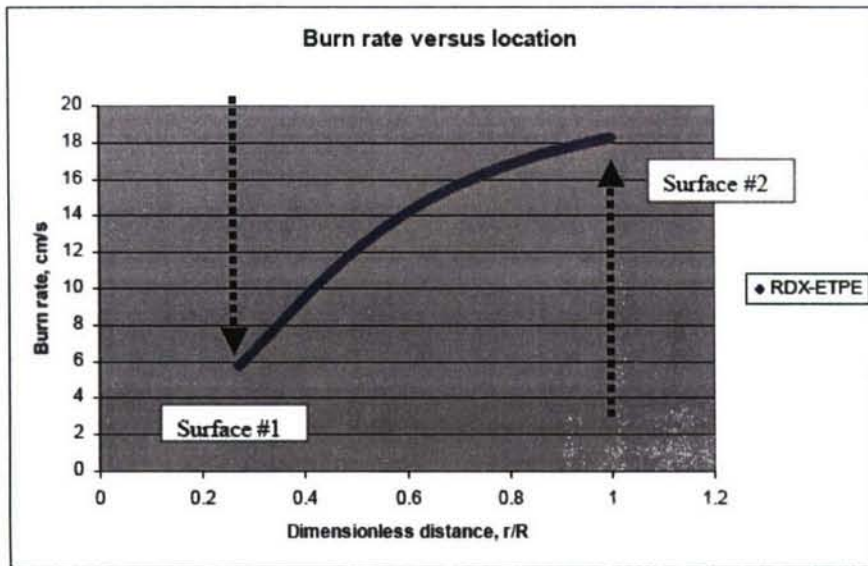


Figure 5

Burn rate versus location in the propellant to be recovered from the annular gap between the two cylinders of figure 4 upon Couette flow

- If a lower ratio of burn rates between the two surfaces is desired, than the rotation of the inner cylinder can be stopped at an appropriately lower number of rotations.
- On the other hand, if a greater ratio of burn rates between the two surfaces is desired one can increase the ratio of the particle radius over the gap in between the two cylinders.
- If the thickness of the propellant grain is to be increased to generate more realistic slabs one would need to decrease the ratio of particle radius over the gap. Here are some typical results expected for different ratios of particle radius to gap at 10000 turns (the model predictions were obtained by using $K_c = 0.43$ and $K_\eta = 0.65$. The non-dimensional inner cylinder radius is $\kappa = 0.2689$ (fig. 6).

Thus, if one uses Class 1 RDX at a volume loading level of 50% RDX with a RDX particle radius of 75 μm , and at a radius, a , over the gap ratio of 0.001, the gap would be 75 mm (about 3 in.) to generate a RDX concentration of 36% by volume at the inner surface and a RDX concentration of 52% at the outer surface of the grain.

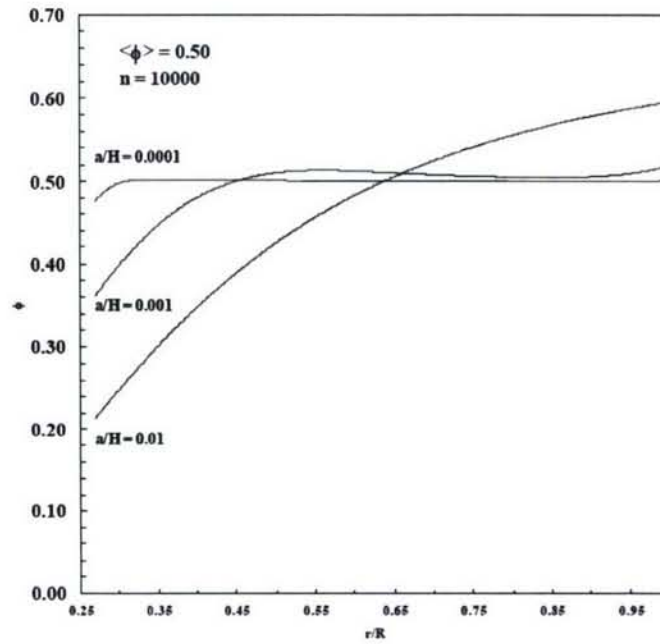


Figure 6

Predicted concentration distribution for a 50% suspension at various particle radius to gap width ratios (results shown are for 10,000 revolutions of the inner cylinder)

Method 2: Generation of Concentration Distributions Using Pressure-Driven Flows through Dies

This is the second option discussed during the meeting at ARDEC on 15 July 2005 and also during the conference call on 4 August 2005. In this method the propellant is forced through a cylindrical tube or a rectangular slit. The typical geometry and the schematics of the flow are shown in figure 7.

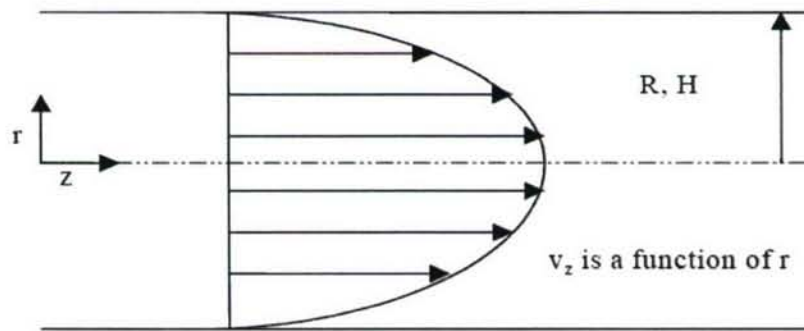


Figure 7

Flow through a rectangular slit of gap, H, or a circular tube with radius R

The equation of conservation of momentum for one-dimensional flow is

$$-\frac{1}{r^s} \frac{d}{dr} (r^s \tau_{rz}) = \frac{dP}{dz} \quad (7)$$

where r is the transverse direction, z is the axial direction, P is the pressure, τ_{rz} is the shearing stress and exponent s is zero for rectangular slit die and one for a cylindrical tube. For simplicity, we will use here the solutions for Poiseuille flow (flow through a circular die) with the caveat that the results are also equally valid for one-dimensional rectangular slit flow and other simple shear flows. The conservation of mass requires:

$$V_z \frac{\partial \phi}{\partial z} = \frac{a^2}{r} \frac{\partial}{\partial r} \left\{ r \left[K_c \left(\phi^2 \frac{\partial \dot{\gamma}}{\partial r} + \dot{\gamma} \phi \frac{\partial \phi}{\partial r} \right) + K_\eta \frac{\dot{\gamma} \phi^2}{\eta_s} \frac{\partial \eta_s}{\partial r} \right] \right\} \quad (8)$$

Equation 8 is solved with the boundary conditions of the total flux being zero at the solid surface

$$K_c \left(\phi^2 \frac{\partial \dot{\gamma}}{\partial r} + \dot{\gamma} \phi \frac{\partial \phi}{\partial r} \right) + K_\eta \frac{\dot{\gamma} \phi^2}{\eta_s} \frac{\partial \eta_s}{\partial r} = 0 \quad (9)$$

and the symmetry condition at the axis of symmetry

$$\frac{\partial \phi}{\partial r} = 0 \quad (10)$$

During the flow of suspensions, a binder-rich apparent slip layer develops with thickness, δ . If this thickness is stable, the relationship between the wall shear stress and slip velocity (Navier's slip condition) is given by the following expression for a Newtonian binder (for $\delta \ll R$)

$$U_s = \frac{\delta}{\eta_o} \tau_w = \beta \tau_w = V_z(R, z) \quad (11)$$

where η_o is the shear viscosity of the Newtonian binder and R is the radius of the capillary. Various techniques are available to determine the Navier's slip coefficient, β , using viscometric flows (refs. 12 through 14).

The particle concentration, ϕ , is assumed to be uniform initially

$$\phi = \phi_o \text{ for } 0 \leq r \leq R \text{ at } z = 0 \quad (12)$$

The resulting coupled set of equations 7 and 8 was solved by Allende and Kalyon (ref. 8) in conjunction with the Krieger (ref. 11) model of the concentration-dependent suspension viscosity using a numerical method. For example, the steady state distributions of the concentration profiles are given in figure 8 for various values of the initial concentration of the solid particles in the range of 10 to 69% by volume (here fully-developed concentration distribution for steady state Poiseuille flow for $K_c / K_\eta = 0.66$ is shown). The fully developed profiles suggest that there would be significant depletion of the particle concentration at the wall of the die and significant increase of the concentration of the particles as one approaches the axis of the symmetry. Thus, under such fully developed conditions one would obtain a significant variation of the particle concentration between the wall and the center.

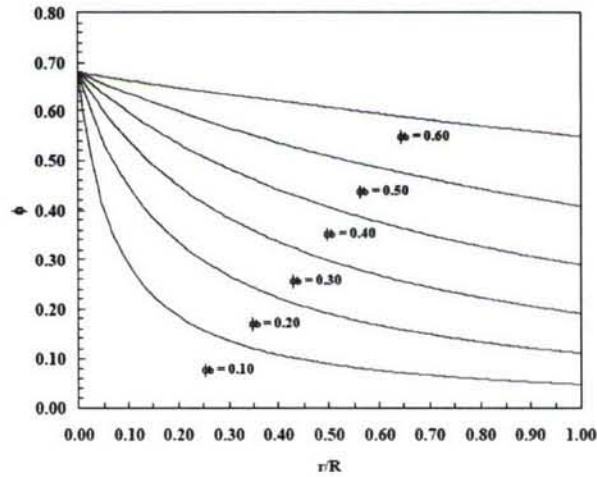


Figure 8
Fully developed concentration distribution for steady state Poiseuille flow

The developments of the concentration distribution in the cylindrical die as a function of the length over the diameter, D , ratio of the die; i.e., L/D are shown next. The initial concentration of the particles is 45% by volume (fig. 9). The ratio of the particle radius to the radius of the tubular die is 0.0256. As the L/D ratio increases, the variations of the concentrations across the gap become more pronounced. Here, the particle concentration distributions for a 45% suspension and a $R = 0.0256$ at various capillary length to diameter ratios are presented. The model predictions were obtained by using $K_c = 0.43$ and $K_\eta = 0.65$.

For example, for a length over diameter ratio of 33, the concentration at the wall is reduced to 0.40 and the concentration of the particles at the axis of symmetry is 0.68. Note the particle radius, a , over the channel radius is 0.0256. Thus, for RDX particles with a radius of 75 μm , the radius of the channel will be 3 mm (diameter of the extrudate will be 6 mm). Then, the total length of the die necessary to achieve this concentration distribution becomes about 200 mm. It should be noted that any increase of the die length over this is advantageous in increasing the concentration gradient of the particles. Thus, the length of the die should be extended as much as possible. If this were a rectangular slit, the gap would be about 6 mm with again a total length of 200 mm.

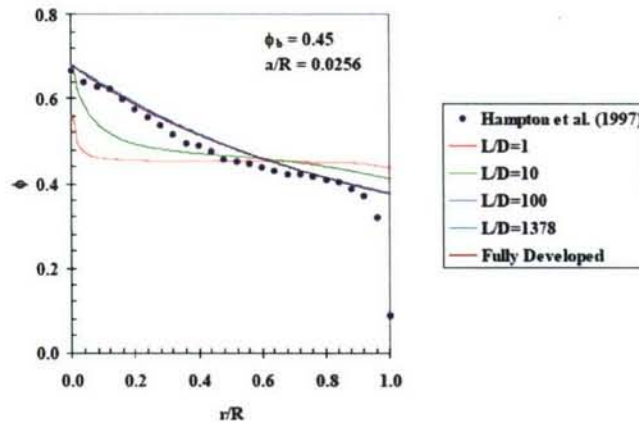


Figure 9
Particle concentration distributions for a 45% suspension and at various capillary length to diameter ratios

SELECTION OF THE BINDER

It is recommended that the binder be Newtonian. There are two possibilities for Newtonian binders:

1. Use a binder, which is thermosetting and cure it at higher temperatures possibly in the die then analyze the section of the material found adjacent to the die exit for gradients and burn rates.
2. Use a binder, which is thermoplastic and quench it upon exit from the die or at the die for demonstration purposes and then analyze the section of the material found adjacent to the die exit for gradients and burn rates.

In the following, one thermosetting material which is inert (green) that we have used is described with the necessary curing catalyst and the curing agent.

EXPERIMENTAL STUDIES USING A SIMULANT AND A SLIT DIE

Materials

The materials of the formulation were the following:

- PS342.5 α, ω -silanol terminated PDMS oil ($M_w = 19,000$ $M_w/M_n = 1.5$) from United Chemical Technologies, Inc.
- 3-M Gray Z-Light ceramic microspheres (G-3500) are low density, fine particle size, hollow microspheres (average particle size is $135 \mu\text{m}$)
- Specific gravity of PDMS 0.97 g/cc and the specific gravity of the ceramic microspheres is 0.7 g/cm^3

- The formulation contains 50% PS342.5 PDMS oil by volume and 50% ceramic hollow microspheres by volume
- The formulation contains 58.1% PS342.5 PDMS oil by weight and 41.9% ceramic hollow microspheres by weight
- For every gram polymer + hollow ceramic microspheres, 60 μ l crosslinking agent (tetraethylorthosilicate, TEOS from Aldrich) and 10 μ l (tin (II) ethylhexanoate from Gelest) were added and premixed

The MSDS sheets and product data for the microspheres were included as the appendix of our report to ARDEC, dated 14 January 2006.

Processing

The formulation was mixed in a high intensity batch mixer with roller blades. The torque as a function of time during the mixing process is shown in figure 10. The torque generated during the mixing process was very small reflecting the low shear viscosity of the binder.

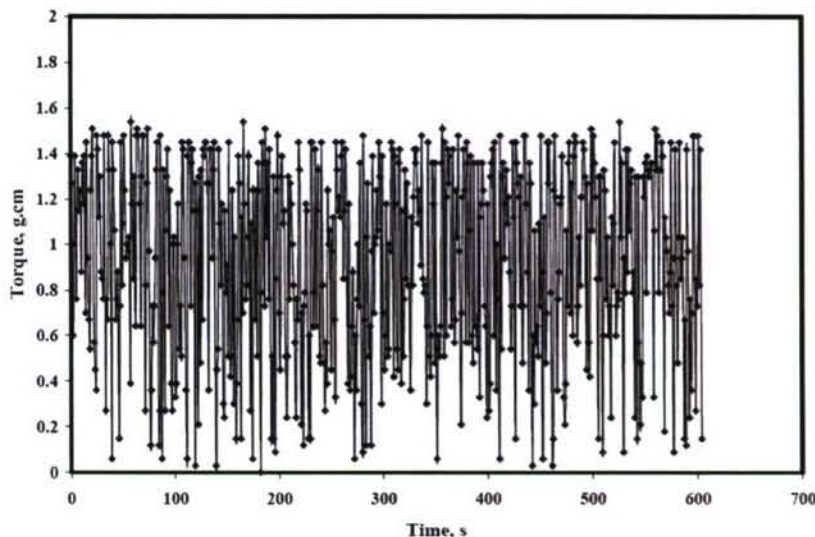


Figure 10

50% PDMS_50% Ceramic microsphere by volume batch mixing at 30 rpm, 210 cm³ for 10 min

Slit Die for Assessing the Migration Effects

The adjustable gap rheometer of SIT was used for the induced flow of the suspension in conjunction with an Instron Floor Model (fig. 11). The suspension was first loaded to a cartridge under vacuum (fig. 12). This unit has an independent drive for loading and may be very useful in the future for the loading of live formulations for rheological testing. The cartridge was then loaded into the slit die rheometer (fig. 13).

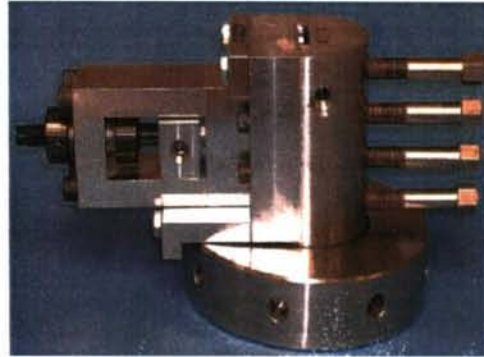
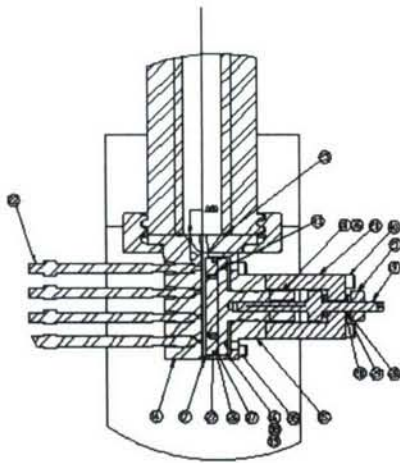


Figure 11
Adjustable gap rheometer (D.M. Kalyon and H. Gokturk, U.S. Patent 5,277,058, 11 Jan 1994)



Figure 12
Cartridge

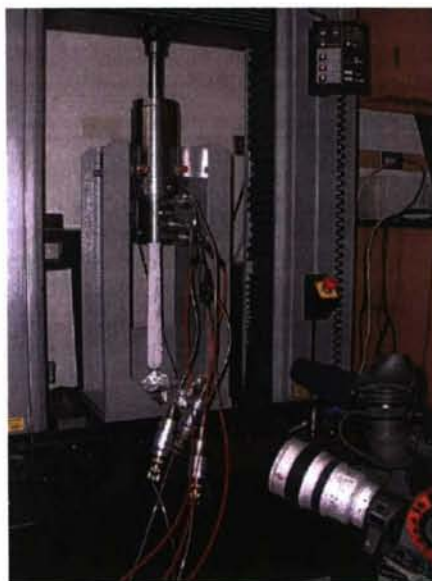


Figure 13
Instron slit rheometer

The flow of the suspension out of the die is shown in figure 14. The suspension had very low elasticity and thus could not hold its shape upon exit from the die (as affected by the Newtonian character of the binder system).



Figure 14
50% PDMS and 50% ceramic microsphere by volume at 0.1 in./min crosshead speed

The crosshead speed used during the extrusion was 0.1 in./min at room temperature. The gap of the slit die was 1.5 mm. The generated steady state force during the extrusion was around 92 lbf.

Collection of the Sample

The flow was brought to a dead stop and the bottom of the slit die was sealed with a Teflon sheet to prevent the leakage of the suspension out of the die exit. The temperature was increased to 80°C for curing.

Upon curing, the splittable slit die was opened removing the sensors located at the walls and the sample was collected. The sample had a tendency to stick to the die walls severely. This was partially alleviated by increasing the concentration of the curing agent to the formulation provided. However, sticking of the formulation is still a problem and precludes the removal of the sample intact from the walls of the slit die. However, parts of the sample could be removed and analyzed.

Microscopy of the Sample and Further Analysis to Follow

The typical optical micrographs of the relatively thick sections of the sample collected (few mm in thickness) are shown in figures 15 through 17. As seen, the relatively thick sections allow the stacking of the spheres on top of each other making it very difficult to determine the concentration distributions of the spheres from one wall to the other. The samples were determined to be suitable for microtoming and scanning electron microscopy, as discussed next.

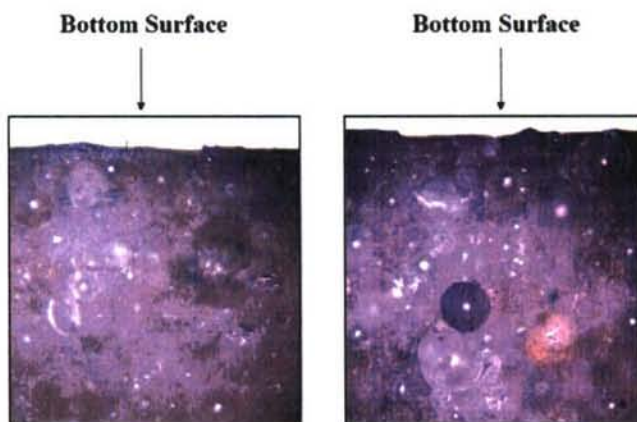


Figure 15
50% PDMS_50% ceramic microsphere by volume

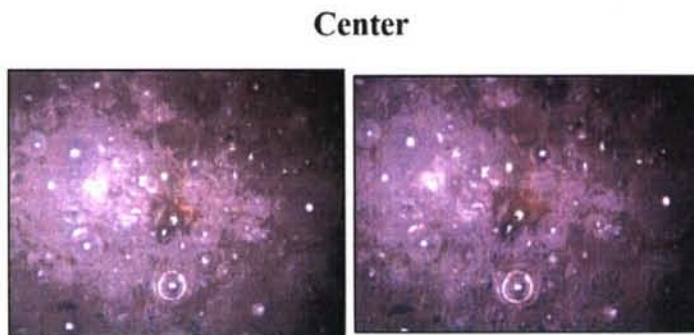


Figure 16
50% PDMS_50% ceramic microsphere by volume

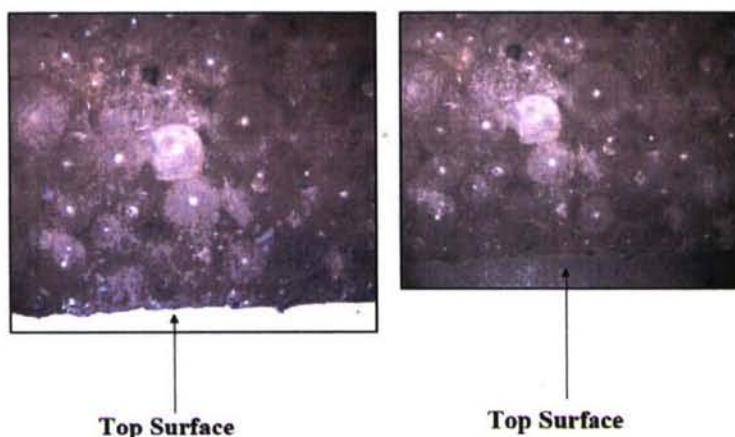


Figure 17
50% PDMS_50% ceramic microsphere by volume

Scanning Electron Microscopy Analysis of the Extruded Samples

The scanning electron micrographs of the various sections of the extrudates are shown in figures 18 to 23. The typical core regions are shown in figures 18 and 19 and indicate that the spheres are well distributed with very little space not occupied by the rigid particles (this includes the space left by the release of the spheres from the surface, the locations of which can be clearly discerned and should be considered as part of the particle occupied regions).

On the other hand, the distributions of particles at the wall regions are very different (figs. 19 to 23). At the wall regions there is a paucity of particles with some zones totally unoccupied by the particles and occupied only by the binder of the suspension; i.e., the PDMS.

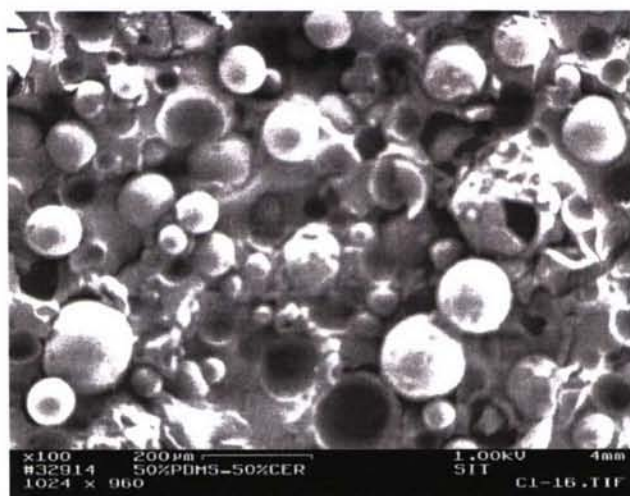


Figure 18
SEM image I - core of the extrudates: away from the wall

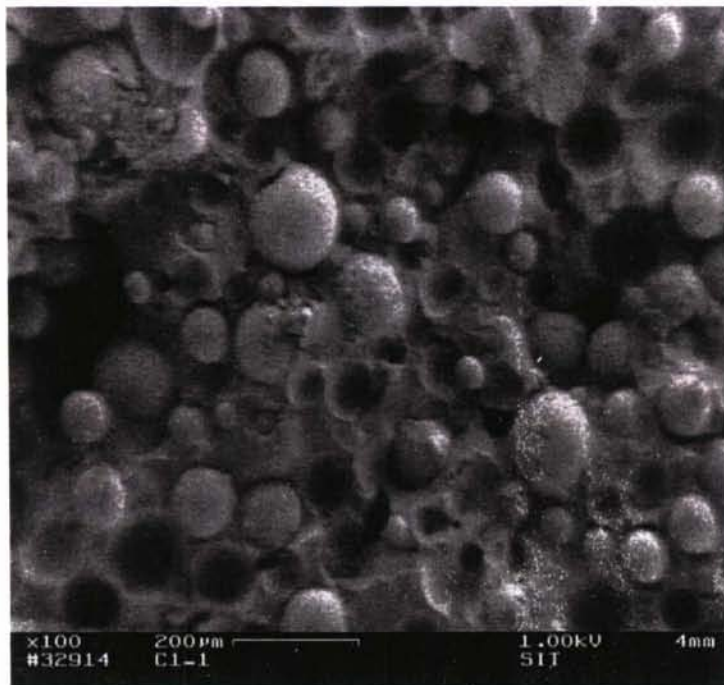


Figure 19
SEM image II - core of the extrudates: away from the wall

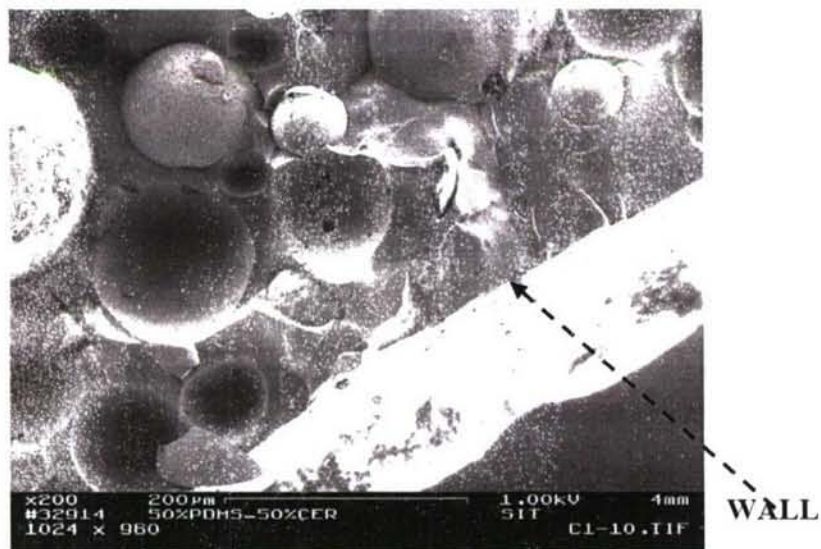


Figure 20
SEM image III - skin of the extrudates: at the wall

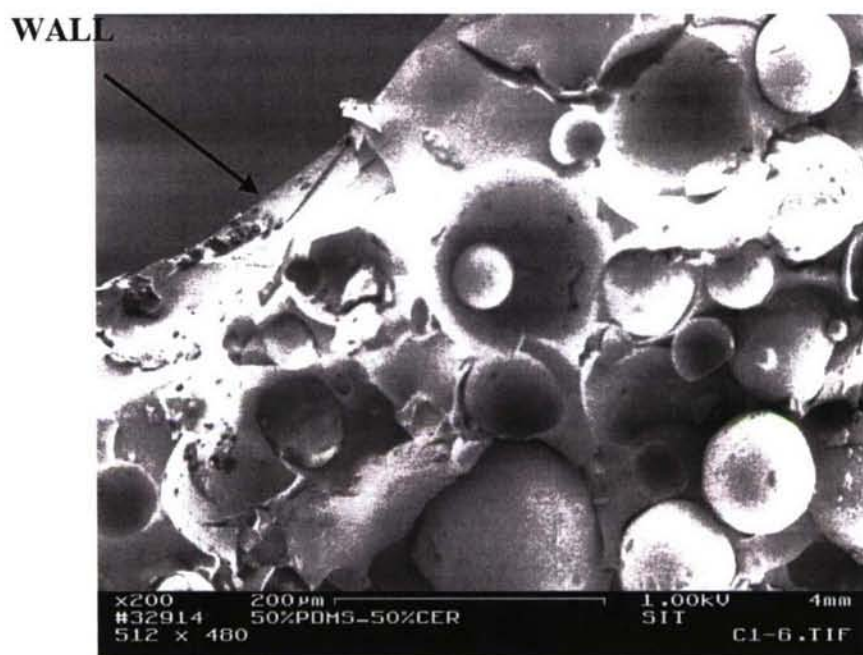


Figure 21
SEM image IV - skin of the extrudates: at the wall

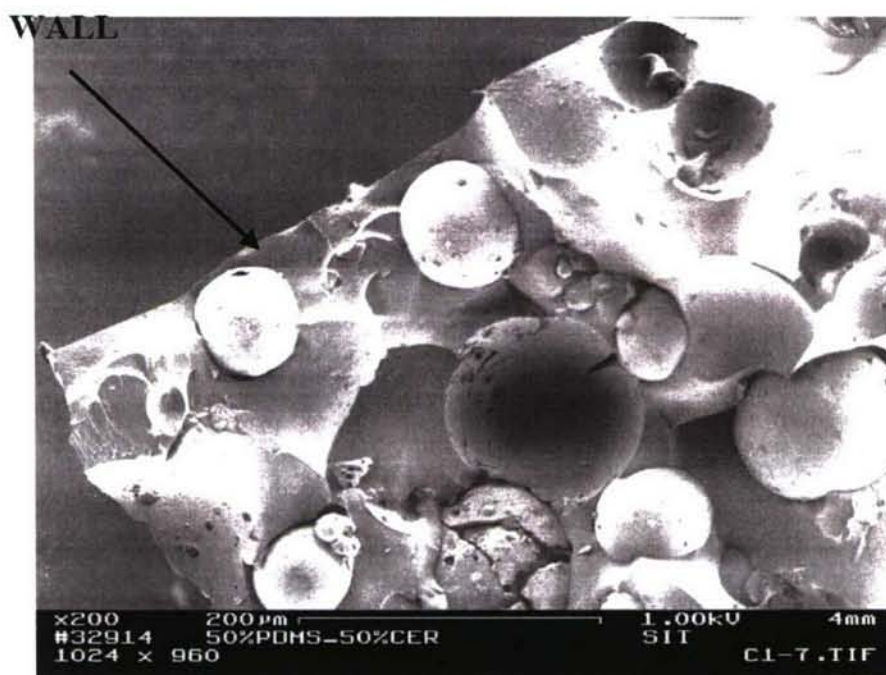


Figure 22
SEM image V - skin of the extrudates: at the wall

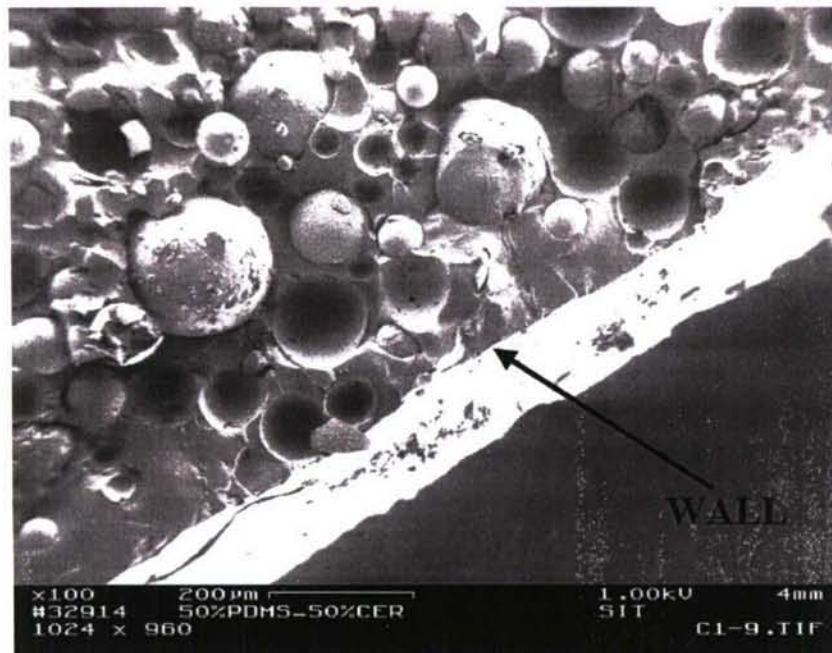


Figure 23
SEM image VI - skin of the extrudates: at the wall

Ramifications

These results indicate that under conditions in which the particle diameter is a relatively high fraction of the gap of the channel, particles will move away from the wall as the theories of shear induced particle migration. Our calculations, as explained earlier, indicate that under such conditions the burn rate will be higher at the core with a slower burn rate at the wall, effectively generating a skin/core composite structure that is functionally graded to generate a burn rate differential across the grain of the propellant.

FUTURE WORK

The preliminary results of the theoretical and experimental work are very interesting and encouraging. However, a lot more work needs to be done to determine the geometries and operating conditions under which such gradation can be controlled and tailored to generate the burn rate differentials that are desired. Furthermore, the promise of the methodology needs to be vindicated by using live suspensions, their extrusion and the structural distributions and burn rate analysis of extruded grains and comparisons with non-graded propellants.

REFERENCES

1. Segré, G. and Silberberg, A., "Radial Particle Displacements in Poiseuille Flow of Suspensions," *Nature* **189**, 209-210, 1961.
2. Goldsmith, H. L. and Mason, S. G., "Axial Migration of Particles in Poiseuille Flow," *Nature* **190**, 1095-1096, 1961.
3. Gadala-Maria, F. and Acrivos, A., "Shear-induced Structure in a Concentrated Suspension of Solid Spheres," *J. Rheol.* **24**, 799-814, 1980.
4. Leighton, D. and Acrivos, A., "The Shear-induced Migration of Particles in Concentrated Suspensions," *J. Fluid Mech.* **181**, 415-439, 1987.
5. Abbott, J. R.; Tetlow, N.; Graham, A. L.; Altobelli, S. A.; Fukushima, E.; Mondy, L. A.; and Stephens, T. S., "Experimental Observations of Particle Migration in Concentrated Suspensions: Couette Flow," *J. Rheol.* **35**, 773-795, 1991.
6. Karnis, A.; Goldsmith, H. L.; and Mason, S. G. Mason, "The Kinetics of Flowing Dispersions. I. Concentrated Suspensions of Rigid Particles," *J. Colloid Interface Sci.* **22**, 531-553, 1966.
7. Koh, C. J.; Hookham, P. Hookham; and Leal, L. G., "An Experimental Investigation of Concentrated Suspension Flows in a Rectangular Channel," *J. Fluid Mech.* **266**, 1-32, 1994.
8. Allende, M. and Kalyon, D., "Assessment of Particle-Migration Effects in Pressure-Driven Viscometric Flows," *J. Rheology*, **44**, 1, 79-90, 2000.
9. Phillips, R. J.; Armstrong, R. C. Armstrong; Brown, R. A. Brown; Graham, A. L. Graham; and Abbott, J. R., "A Constitutive Equation for Concentrated Suspensions that Accounts for Shear-induced Particle Migration," *Phys. Fluids A* **4**, 30-40, 1992.
10. Homan, B.; Devynck, D. Devynck; Kaste, P. Kaste; Lieb, R. Lieb; Bullock, D.; and Juhasz, A., "BNMO/NMMO/RDX TPE Propellant Performance as a Function of Nitramine Particle Size and Solids Loading," Technical Report ARL-TR-2624, U.S. Army Research Laboratory, December 2001.
11. Krieger, I. M., "Rheology of Monodisperse Lattices," *Adv. Colloid Interface Sci.* **3**, 111-136, 1972.
12. Allende, M., "Shear Induced Particle Migration in Suspensions of Non-colloidal Particles", PhD Thesis, Stevens Institute of Technology, Hoboken, NJ, 2000.
13. Kalyon, D. M.; Yaras, P.; Aral, B.; and Yilmazer, U., "Rheological Behavior of a Concentrated Suspension: A Solid Rocket Fuel Simulant," *J. Rheol.* **37**, 35-53, 1993.

14. Aral, B. K. and Kalyon, D. M., "Effects of Temperature and Surface Roughness on Time-dependent Development of Wall Slip in Steady Torsional Flow of Concentrated Suspensions," J. Rheol. **38**, 957-972, 1994.
15. Yilmazer, U. and Kalyon, D. M., "Slip Effects in Capillary and Parallel Disk Torsional Flows of Highly Filled Suspensions," J. Rheol. **33**, 1197-1212 (1989).

DISTRIBUTION LIST

U.S. Army ARDEC

ATTN: AMSRD-AAR-EMK

AMSRD-AAR-GC

AMSRD-AAR-AEE-W, P. Hui

A. Eng

T. Manning

D. Park

E. Rozumou

D. Fair (5)

AMSRD-AAR-AEE-P, L. Sotsky

S. Moy (2)

D. Chiu (2)

AMSRD-AAR-AE, A. Perich

Picatinny Arsenal, NJ 07806-5000

Defense Technical Information Center (DTIC)

ATTN: Accessions Division

8725 John J. Kingman Road, Ste 0944

Fort Belvoir, VA 22060-6218

Commander

Soldier and Biological/Chemical Command

ATTN: AMSSB-CII, Library

Aberdeen Proving Ground, MD 21010-5423

Director

U.S. Army Research Laboratory

ATTN: AMSRL-CI-LP, Technical Library

Bldg. 4600

Aberdeen Proving Ground, MD 21005-5066

Chief

Benet Weapons Laboratory, AETC

U.S. Army Research, Development and Engineering Command

Armament Research, Development and Engineering Center

ATTN: AMSRD-AAR-AEW

Watervliet, NY 12189-5000

Director

U.S. Army TRADOC Analysis Center-WSMR

ATTN: ATRC-WSS-R

White Sands Missile Range, NM 88002

Chemical Propulsion Information Agency

ATTN: Accessions

10630 Little Patuxent Parkway, Suite 202

Columbia, MD 21044-3204

GIDEP Operations Center
P.O. Box 8000
Corona, CA 91718-8000

U.S. Army Research Laboratory
ATTN: AMSRD-ARL-WM-RD, J. Colburn
N. Eldredge
Aberdeen Proving Ground, MD 21005-5066

Commander
NSWC
Indian Head Division
ATTN: C. Michienzi
R. Mascardo
R.J. Cramer
101 Strauss Avenue
Indian Head, MD 20640